Supplementary material for "Two-dimensional conical dispersion in $ZrTe_5$ evidenced by optical spectroscopy"

E. Martino,[1,*] I. Crassee,[2,*] G. Eguchi,[3] D. Santos-Cottin,[4] R.D. Zhong,[5] G.D. Gu,[5] H. Berger,[6] Z. Rukelj,[7] M. Orlita,[8,9] C. C. Homes,[5] and Ana Akrap[4,†]

[1] *IPHYS, EPFL, CH-1015 Ecublens, Switzerland*
[2] *LNCMI, CNRS-UGA-UPS-INSA, 25, avenue des Martyrs, F-38042 Grenoble, France*
[3] *Institute of Solid State Physics, Vienna University of Technology, Wiedner Hauptstrasse 8-10, 1040 Vienna, Austria*
[4] *University of Fribourg, Switzerland*
[5] *Condensed Matter Physics and Materials Science Department, Brookhaven National Laboratory, Upton, New York 11973, USA*
[6] *EPFL, CH-1015 Ecublens, Switzerland*
[7] *Department of Physics, Faculty of Science, University of Zagreb, Bijenička 32, HR-10000 Zagreb, Croatia*
[8] *LNCMI, CNRS-UGA-UPS-INSA-EMFL, 25, avenue des Martyrs, F-38042 Grenoble, France*
[9] *Institute of Physics, Charles University in Prague, CZ-12116 Prague, Czech Republic*

(Dated: May 1, 2019)

In the Supplementary Materials we show the two-band analysis of the magneto-transport data. We continue with the derivation of the interband conductivity for a 2D Dirac cone with a parabolic z dispersion. We explain the definition of the spectral weight applied in the main text. Further, we present a comparison of the experimental optical conductivity and the conductivity determined from a density functional theory band calculation. Finally, we show how one can determine the optical gap from the reflectance spectrum.

TWO-BAND ANALYSIS OF MAGNETO-TRANSPORT DATA

In the main text we show a single-band analysis of the magneto-transport results on single crystals of $ZrTe_5$. This approach shows that the carrier density varies non-monotonically with temperature. The carrier density is minimal at an intermediate, sample-dependent temperature T', the same temperature at which the sign of the majority carriers switches from high-temperature hole-like to low-temperature electron-like carriers.

The goal here is to show how the total carrier density n, Hall mobility μ_H and the dc conductivity σ_{xx} can be decomposed using a carefully controlled two-component analysis. In this picture, the two components are an outcome of the analysis at each temperature, and they are an electron-like band and a hole-like band, separated by a band gap of $2\Delta = 6$ meV. The analysis approach is described in the Ref. 1. The results of such a two-component analysis are shown in Fig. S1 (a–c) for sample A, and in panels (d–f) for sample B.

At the lowest temperature ($T = 2$ K), the contribution to the conductivity is dominated by high-mobility electron-like carriers. The minority carriers from the hole-like band contribute very little to the conductivity: less than 1% in sample A, and about 4% in sample B. Similarly, at room temperature, the conductivity is dominated by hole-like carriers. This confirms that at very low temperatures, and at room temperature, a single band is sufficient to describe the transport properties.

In the intermediate range of temperatures, and in particular between 50 and 100 K, the contributions of the two bands become comparable and also more difficult to separate (resulting in larger error bars). Between room temperature and T', the carrier density and the Hall mobility of the majority carriers have a temperature dependence which is characteristic of thermally excited carriers. This is in agreement with the chemical potential being inside the band gap whose size is smaller than the thermal energy of the carriers. The minority component has a weak temperature dependence of the mobility, characteristic of a metallic contribution.

INTERBAND CONDUCTIVITY FOR A 2D DIRAC CONE WITH A PARABOLIC z-DISPERSION

A simple two band Hamiltonian is presented with four free parameters. Optical conductivity, single band density of state and low energy form of the electron dispersions are calculated from the model and used in obtaining values that can be compared to the experimental results. The free parameters of the proposed Hamiltonian can in this way be unambiguously determined.

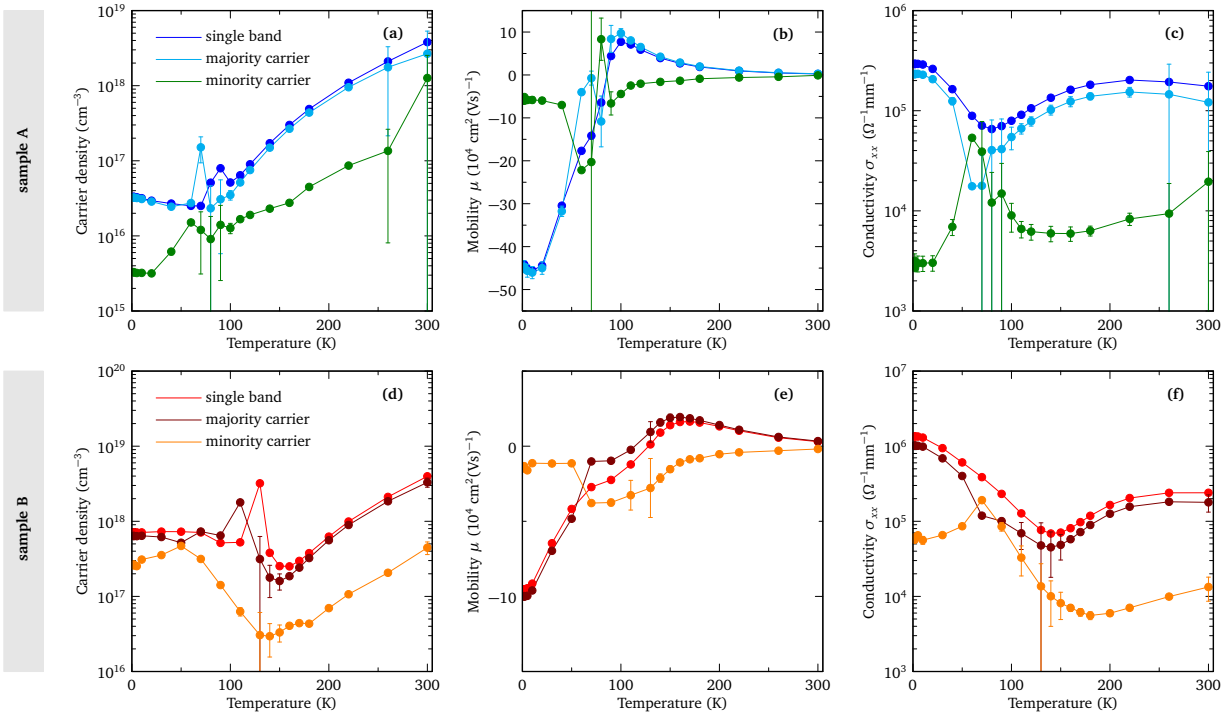

Fig. S1. Carrier density, mobility, and conductivity obtained in a two-band analysis as discussed in the text.

Hamiltonian

Here we present a posible two band electron model with the quasi-Dirac features in the vicinity of the Γ point in the Brillouin zone. It phenomenologically implements the energy band gap 2Δ originating from the spin-orbit coupling, with the assumption of a free-electron like behaviour in the z direction. The Hamiltonian is

$$H = \begin{pmatrix} \Delta + \zeta k_b^2 & \hbar v_a k_a - i\hbar v_c k_c \\ \hbar v_a k_a + i\hbar v_c k_c & -\Delta - \zeta k_b^2 \end{pmatrix}. \tag{S1}$$

The elements v_α are the Dirac velocities in the a and c direction and $\zeta = \hbar^2/2m^*$ with m^* being the effective mass. These parameters can be unambiguously determined by comparing the experimental data from the optical and transport measurement on a clean $ZrTe_5$ sample and the predictions derived from the above Hamiltonian. The eigenvalues of the Hamiltonian (S1) are

$$\varepsilon_{2,1\mathbf{k}} = \pm\sqrt{\hbar^2(v_a k_a)^2 + \hbar^2(v_c k_c)^2 + (\Delta + \zeta k_b^2)^2}. \tag{S2}$$

and are symmetrical to one another with respect to the band gap middle. Since conduction band $\varepsilon_{2\mathbf{k}}$ is weakly filled we can expand (S2) to the $\mathcal{O}(k^2)$

$$\varepsilon_{2\mathbf{k}} \approx \Delta + \frac{(\hbar v_a)^2}{2\Delta}k_a^2 + \frac{(\hbar v_c)^2}{2\Delta}k_c^2 + \frac{\hbar^2}{2m^*}k_b^2, \tag{S3}$$

thus obtaining the effective masses

$$m_{aa} = \Delta/v_a^2,\ m_{cc} = \Delta/v_c^2,\ m_{bb} = m^* \tag{S4}$$

Interband conductivity

The interband conductivity tensor $\sigma^\alpha(\omega, T)$ in the relaxation constant approximation Γ is given in the usual way

$$\sigma^\alpha(\omega, T) = \frac{i\hbar}{V}\sum_{\mathbf{k}\sigma L\neq\underline{L}} \frac{\left|J^{L\underline{L}}_{\alpha\mathbf{k}}\right|^2}{\varepsilon_{\underline{L}\mathbf{k}} - \varepsilon_{L\mathbf{k}}} \frac{f_{L\mathbf{k}} - f_{\underline{L}\mathbf{k}}}{\hbar\omega + \varepsilon_{L\mathbf{k}} - \varepsilon_{\underline{L}\mathbf{k}} + i\Gamma_{\underline{L}L}} \tag{S5}$$

where $\alpha \in \{a, c, b\}$ is a Cartesian coordinate and $J^{LL}_{\alpha\mathbf{k}}$ are the interband current vertices calculated further below. Now we can calculate the interband conductivity in the a direction in the case of vanishing relaxation constant $\Gamma_{12} \to 0$. Using the derived value $|J_{a\mathbf{k}}|^2 = e^2 v_a^2$ and taking only the positive values of $\Omega = \hbar\omega$, the real part of (S5) reduces to

$$\sigma_1^a(\Omega, T) = \hbar e^2 v_a^2 \pi \frac{1}{V} \sum_{\mathbf{k}\sigma} \frac{f_{1\mathbf{k}} - f_{2\mathbf{k}}}{\varepsilon_{2\mathbf{k}} - \varepsilon_{1\mathbf{k}}} \delta(\Omega - \varepsilon_{2\mathbf{k}} + \varepsilon_{1\mathbf{k}}). \tag{S6}$$

The temperature dependence is implemented in the Fermi-Dirac distribution. Taking into account that $\varepsilon_{2\mathbf{k}} = -\varepsilon_{1\mathbf{k}}$ and that the expresion (S6) is finite only for $\Omega = \varepsilon_{2\mathbf{k}} - \varepsilon_{1\mathbf{k}}$, the distribution functions can be written

$$\begin{aligned} F(\Omega, T) = f_{1\mathbf{k}} - f_{2\mathbf{k}} &= \frac{1}{e^{\beta(-\Omega/2-\mu)} + 1} - \frac{1}{e^{\beta(\Omega/2-\mu)} + 1} \\ &= \frac{\mathrm{sh}(\beta\Omega/2)}{\mathrm{ch}(\beta\mu) + \mathrm{ch}(\beta\Omega/2)} \underset{T=0}{\longrightarrow} \Theta(\Omega - 2\varepsilon_F) \end{aligned} \tag{S7}$$

Next, we introduce the new variables $2v_a\hbar k_a = x$, $2v_c\hbar k_c = y$ and $k_b\sqrt{2\zeta} = z$. Thus (S6) becomes

$$\sigma_1^a(\Omega, T) = \frac{\hbar e^2 v_a^2 \pi}{(2\pi)^3} \frac{F(\Omega, T)}{(2v_a\hbar)(2v_c\hbar)} \frac{2}{\sqrt{2\zeta}} \iiint \frac{\delta\left(\Omega - \sqrt{x^2 + y^2 + (2\Delta + z^2)^2}\right)}{\sqrt{x^2 + y^2 + (2\Delta + z^2)^2}} dxdydz \tag{S8}$$

Changing the Cartesian to the cyllindrical system by introducing $\varrho^2 = x^2 + y^2$ (S8) is

$$\sigma_1^a(\Omega, T) = \frac{\hbar e^2 v_a^2 \pi}{(2\pi)^3} \frac{F(\Omega, T)}{(2v_a\hbar)(2v_c\hbar)} \frac{4\pi}{\sqrt{2\zeta}} \int_0^\infty \int_{-\infty}^\infty \frac{\delta\left(\Omega - \sqrt{\varrho^2 + (2\Delta + z^2)^2}\right)}{\sqrt{\varrho^2 + (2\Delta + z^2)^2}} \varrho d\varrho dz \tag{S9}$$

We note that there are two zeros of z argument within the δ function $z_0 = \pm\sqrt{\sqrt{\Omega^2 - \varrho^2} - 2\Delta}$. This gives an extra factor of 2

$$\sigma_1^a(\Omega, T) = \frac{\hbar e^2 v_a^2 \pi}{(2\pi)^3} \frac{F(\Omega, T)}{(2v_a\hbar)} \frac{1}{(2v_c\hbar)} \frac{8\pi}{\sqrt{2\zeta}} \int_0^{\sqrt{\Omega^2 - 4\Delta^2}} \frac{\varrho d\varrho}{\sqrt{\Omega^2 - \varrho^2}\sqrt{\sqrt{\Omega^2 - \varrho^2} - 2\Delta}} \tag{S10}$$

The integral is equal to $2\sqrt{\Omega - 2\Delta}$, giving the final result for the interband conductivity in terms of $\sigma_0 = e^2/(4\hbar)$ for $T = 0$

$$\sigma_1^a(\Omega, 0) = \frac{\sigma_0}{\pi} \frac{v_a}{v_c} \frac{\sqrt{m^*}}{\hbar} \sqrt{\Omega - 2\Delta}\ \Theta(\Omega - 2\varepsilon_F), \tag{S11}$$

The derivation of $\sigma_1^a(\Omega)$ is esentialy the same, the only difference is the current vertex (S37). This gives

$$\sigma_1^c(\Omega, 0) = \frac{\sigma_0}{\pi} \frac{v_c}{v_a} \frac{\sqrt{m^*}}{\hbar} \sqrt{\Omega - 2\Delta}\ \Theta(\Omega - 2\varepsilon_F) \tag{S12}$$

Using (S11) and (S12) we are at liberty to write the second prediction of our model

$$\frac{\sigma_1^a(\Omega, 0)}{\sigma_1^c(\Omega, 0)} = \frac{v_a^2}{v_c^2} \tag{S13}$$

Density of states

The single band density of state is defined

$$g(\varepsilon) = \frac{1}{V} \sum_{\mathbf{k}\sigma} \delta(\varepsilon - \varepsilon_{2\mathbf{k}}) \tag{S14}$$

Using the eigenvalues (S2) and the procedure outlined in (S8)-(S11) we obtain

$$g(\varepsilon) = \frac{1}{\pi^2\hbar^3}\frac{1}{v_a v_c}\sqrt{2m^*}\,\varepsilon\sqrt{\varepsilon-\Delta} \tag{S15}$$

Now, the connection to the concentration of electrons can be made. For $T = 0$ we have

$$n = \int_{\Delta}^{\varepsilon_F} g(\varepsilon)d\varepsilon = \frac{1}{\pi^2\hbar^3}\frac{1}{v_a v_c}\sqrt{2m^*}\frac{2}{15}(\varepsilon_F-\Delta)^{3/2}(2\Delta+3\varepsilon_F). \tag{S16}$$

Effective number of charge carriers and the plasmon frequency

The effective concentration of charge carriers $n_{\alpha\alpha}$ is defined

$$n_\alpha = -\frac{1}{V}\sum_{\mathbf{k}\sigma} m_e v_{\alpha\mathbf{k}}^2 \frac{\partial f_{\mathbf{k}}}{\partial\varepsilon_{\mathbf{k}}}, \tag{S17}$$

where $v_{\alpha\mathbf{k}} = (1/\hbar)\partial\varepsilon_{\mathbf{k}}/\partial k_\alpha$. Choosing $\alpha = a$, for low temperatures ($T \approx 0$) we have $\partial f_{\mathbf{k}}/\partial\varepsilon_{\mathbf{k}} = -\delta(\varepsilon_F - \varepsilon_{\mathbf{k}})$. Using the dispersion (S3) in expression (S17) we have

$$n_a = \frac{1}{(2\pi)^3}2m_e\frac{\hbar^2}{m_{aa}^2}\frac{2m_{aa}}{\hbar^2}\frac{\sqrt{2m_{aa}2m_{cc}2m_{bb}}}{\hbar^3}\iiint x^2\delta(\varepsilon_F-\Delta-x^2-y^2-z^2)dx\,dy\,dz \tag{S18}$$

with the redefined variables $x^2 = (\hbar^2/2m_{aa})k_a^2$, $y^2 = (\hbar^2/2m_{cc})k_c^2$ and $z^2 = (\hbar^2/2m_{bb})k_b^2$. Changing from the Cartesian to the cyllindrical system we obtain

$$n_a = \frac{2}{(2\pi)^3}\frac{m_e}{m_{aa}}\frac{\sqrt{2m_{aa}2m_{cc}2m_{bb}}}{\hbar^3}\int_0^\infty\int_0^{2\pi}\varrho^3\cos^2\varphi\,\delta(\varepsilon_F-\Delta-\varrho^2-z^2)d\varrho\,d\varphi\,dz. \tag{S19}$$

Evaluating the δ function integral in the standard way

$$n_a = \frac{4}{(2\pi)^3}\frac{m_e}{m_{aa}}\frac{\sqrt{2m_{aa}2m_{cc}2m_{bb}}}{\hbar^3}\int_0^{\sqrt{\varepsilon_F-\Delta}}\int_0^{2\pi}\frac{\varrho^3\cos^2\varphi}{\sqrt{\varepsilon_F-\Delta-\varrho^2}}d\varrho\,d\varphi, \tag{S20}$$

gives us the final result

$$n_a = \frac{1}{(2\pi)^2}\frac{4}{3}(\varepsilon_F-\Delta)^{3/2}\frac{m_e}{m_{aa}}\frac{\sqrt{2m_{aa}2m_{cc}2m_{bb}}}{\hbar^3}. \tag{S21}$$

By implementing the effective masses (S4) in (S21) we find the effective concentration of charge carriers

$$n_a = 1.06\times10^{25}\,\mathrm{m}^{-3} \gg n = 3\times10^{22}\,\mathrm{m}^{-3} \tag{S22}$$

to be three orders of magnitude larger than n. In the system with the electron bands described by (S3) one has

$$\frac{n_\alpha}{m_e} = \frac{n}{m_{\alpha\alpha}}. \tag{S23}$$

The bare plasmon energy can now be calculated

$$E_{pl} = \hbar\omega_{pl} = \hbar\sqrt{\frac{e^2 n_a}{\epsilon_0 m_e}} = 0.12\,\mathrm{eV} = 970\,\mathrm{cm}^{-1} \tag{S24}$$

and compared with the conductivity sum rule for sample A.

Finite temperature effects

In metals due to finite temperatures the deviations of the chemical potential μ from ε_F is

$$\mu \approx \varepsilon_F \left[1 - \frac{\pi^2}{6}\frac{(k_BT)^2}{\varepsilon_F}\frac{1}{g(\varepsilon)}\frac{\partial g(\varepsilon)}{\partial \varepsilon}\bigg|_{\varepsilon_F}\right] \tag{S25}$$

or inserting (S15) in (S25)

$$\mu \approx \varepsilon_F \left[1 - \frac{\pi^2(k_BT)^2}{12\varepsilon_F^2}\frac{3\varepsilon_F - 2\Delta}{\varepsilon_F - \Delta}\right]. \tag{S26}$$

This alters the effective concentration (S21) in a trivial way

$$\begin{aligned} n_a(T) &= \frac{1}{(2\pi)^2}\frac{4}{3}(\mu-\Delta)^{3/2}\frac{m_e}{m_{aa}}\frac{\sqrt{2m_{aa}2m_{cc}2m_{bb}}}{\hbar^3} \\ &\approx n_a(0)\left(1 - \frac{\pi^2}{8}\frac{(k_BT)^2}{(\varepsilon_F-\Delta)^2}\frac{3\varepsilon_F-2\Delta}{\varepsilon_F}\right) \end{aligned} \tag{S27}$$

From the definition of Drude DC conductivity with scattering time τ

$$\rho_a(T) = 1/\sigma_1^a(T) = \frac{m_e}{e^2\tau n_a(T)} \approx \frac{m_e}{e^2\tau n_a(0)}\left(1 + \frac{\pi^2}{8}\frac{(k_BT)^2}{(\varepsilon_F-\Delta)^2}\frac{3\varepsilon_F-2\Delta}{\varepsilon_F}\right) = \rho_a(0) + AT^2 \tag{S28}$$

with the constant $A = 0.66\times 10^{-9}\Omega\mathrm{m/K}^2$.

Interband current vertices

In the general form of the 2×2 hamiltonian

$$H = \begin{pmatrix} D_{\mathbf{k}} & t_{\mathbf{k}} \\ t_{\mathbf{k}}^* & Q_{\mathbf{k}} \end{pmatrix} \tag{S29}$$

the current vertices are

$$J_{\alpha\mathbf{k}}^{LL'} = \sum_{\ell\ell'}\frac{e}{\hbar}\frac{\partial H_{\mathbf{k}}^{\ell\ell'}}{\partial k_\alpha}U_{\mathbf{k}}(\ell,L)U_{\mathbf{k}}^*(\ell',L') \tag{S30}$$

where $U_{\mathbf{k}}(\ell,L)$ are the elements of matrix defined as $\mathbf{U}\hat{H}\mathbf{U}^{-1} = \mathbf{E}$ and are explicitly given

$$U_{\mathbf{k}}(\ell,L) = \begin{pmatrix} e^{i\varphi_{\mathbf{k}}}\cos(\vartheta_{\mathbf{k}}/2) & e^{i\varphi_{\mathbf{k}}}\sin(\vartheta_{\mathbf{k}}/2) \\ -\sin(\vartheta_{\mathbf{k}}/2) & \cos(\vartheta_{\mathbf{k}}/2) \end{pmatrix} \tag{S31}$$

with the definitions

$$t_{\mathbf{k}} = |t_{\mathbf{k}}|e^{i\varphi_{\mathbf{k}}}, \quad \tan\varphi_{\mathbf{k}} = \frac{\Im t_{\mathbf{k}}}{\Re t_{\mathbf{k}}}, \quad \tan\vartheta_{\mathbf{k}} = \frac{2|t_{\mathbf{k}}|}{D_{\mathbf{k}} - Q_{\mathbf{k}}}. \tag{S32}$$

Therefore in the general case of (S29), equation (S30) gives

$$\frac{\hbar}{e}J_{\alpha\mathbf{k}}^{12} = \frac{\tan\vartheta_{\mathbf{k}}}{2\sqrt{1+\tan^2\vartheta_{\mathbf{k}}}}\frac{\partial(D_{\mathbf{k}}-Q_{\mathbf{k}})}{\partial k_\alpha} + i|t_{\mathbf{k}}|\frac{\partial\varphi_{\mathbf{k}}}{\partial k_\alpha} + \frac{1}{\sqrt{1+\tan^2\vartheta_{\mathbf{k}}}}\frac{\partial|t_{\mathbf{k}}|}{\partial k_\alpha} \tag{S33}$$

Let us now determine the above derivations for the Hamiltonian (S1). We obtain

$$\frac{\partial|t_{\mathbf{k}}|}{\partial k_\alpha} = \hbar\frac{v_a^2k_a\delta_{\alpha,a} + v_c^2k_c\delta_{\alpha,c}}{\sqrt{(v_ak_a)^2+(v_ck_c)^2}} \tag{S34}$$

and

$$\frac{\partial\varphi_{\mathbf{k}}}{\partial k_\alpha}=\frac{v_a v_c(k_a\delta_{\alpha,c}-k_c\delta_{\alpha,a})}{(v_a k_a)^2+(v_c k_c)^2} \tag{S35}$$

and trivialy

$$\frac{\partial(D_{\mathbf{k}}-Q_{\mathbf{k}})}{\partial k_\alpha}=4\zeta k_b\delta_{\alpha,b}. \tag{S36}$$

We are interested in the behaviour in the vicinity of the Dirac point. In this case $(k_a,k_c,k_b)\to 0$ and thus $\tan\vartheta_{\mathbf{k}}\to 0/\Delta=0$. Then inserting (S35) and (S34) in (S33) for the $\alpha=c$ polarization we have

$$J_{c\mathbf{k}}\approx\frac{e(iv_a v_c k_a+v_c^2 k_c)}{\sqrt{(v_a k_a)^2+(v_c k_c)^2}}\to|J_{c\mathbf{k}}|^2=e^2v_c^2. \tag{S37}$$

On similar grounds we obtain for the case $\alpha=a$

$$|J_{a\mathbf{k}}|^2=e^2v_a^2. \tag{S38}$$

Slightly more complicated result is obtained for the b direction which gives

$$|J_{b\mathbf{k}}|^2=4e^2\zeta^2\frac{(v_a k_a)^2+(v_c k_c)^2}{\varepsilon_{\mathbf{k}}^2} \tag{S39}$$

Interaction with magnetic field

We consider the problem of $ZrTe_5$ in uniform magnetic field applied in z direction. We chose the Landau gauge $\mathbf{A}=-By\hat{x}$. It is easy to verify that $\nabla\times\mathbf{A}=B\hat{z}$. The minimal substitution modifies the electron momentum operator $\hat{\mathbf{p}}\to\hat{\mathbf{p}}+e\mathbf{A}$, or by components $\hat{p}_x\to\hat{p}_x+eBy$, $\hat{p}_y\to\hat{p}_y$, $\hat{p}_z\to\hat{p}_z$. Let us write the Hamiltonian (S1) in x,y,z coordinates

$$H=\begin{pmatrix}\Delta+\zeta k_z^2 & \hbar v_x k_x-i\hbar v_y k_y\\ \hbar v_x k_x+i\hbar v_y k_y & -\Delta-\zeta k_z^2\end{pmatrix}. \tag{S40}$$

Then using de Broglie relation $\mathbf{p}=\hbar\mathbf{k}$ and coordinate representation of the momentum operator, the H_{12} term of (S40) in magnetic field is transformed $H_{12}\to\tilde{H}_{12}$

$$\begin{aligned}H_{12}=&\hbar v_x k_x-i\hbar v_y k_y\\ &=v_x p_x-iv_y p_y\to v_x(p_x-eBy)-iv_y\hbar\frac{\partial}{\partial y}\\ \tilde{H}_{12}=&\hbar\sqrt{v_x v_y}\left(\sqrt{\frac{v_x}{v_y}}k_x-\sqrt{\frac{v_x}{v_y}}\frac{eB}{\hbar}y-\sqrt{\frac{v_y}{v_x}}\frac{\partial}{\partial y}\right)\\ &=\frac{\hbar}{\ell}\sqrt{v_x v_y}\left(\gamma\ell k_x+\frac{\gamma}{\ell}y-\frac{\ell}{\gamma}\frac{\partial}{\partial y}\right),\end{aligned} \tag{S41}$$

where we have defined the length scale $\ell=\sqrt{\hbar/(eB)}$ and ratio $\gamma=\sqrt{v_x/v_y}$. Similar result is derived for $\tilde{H}_{21}$. Let us introduce $\eta=\gamma\ell k_x-(\gamma/\ell)y$, then using the chain rule $\partial_\eta=-(\ell/\gamma)\partial_y$, (S40) is

$$\tilde{H}=\begin{pmatrix}\Delta+\zeta k_z^2 & (\hbar/\ell)\sqrt{v_x v_y}\,(\eta+\partial_\eta)\\ (\hbar/\ell)\sqrt{v_x v_y}\,(\eta-\partial_\eta) & -\Delta-\zeta k_z^2\end{pmatrix}. \tag{S42}$$

Defining raising $\hat{a}^\dagger=1/\sqrt{2}\,(\eta-\partial_\eta)$ and lowering $\hat{a}=1/\sqrt{2}\,(\eta+\partial_\eta)$ operator we write (S42)

$$\tilde{H}=\begin{pmatrix}\Delta+\zeta k_z^2 & (\hbar/\ell)\sqrt{2v_x v_y}\hat{a}\\ (\hbar/\ell)\sqrt{2v_x v_y}\hat{a}^\dagger & -\Delta-\zeta k_z^2\end{pmatrix}. \tag{S43}$$

Diagonalization of the above Hamiltonian is straight forward, using the definition of the number operator $\hat{a}^\dagger\hat{a}=\mathcal{N}$ we obtain

$$\tilde{\varepsilon}_{B,k}=\pm\sqrt{2\hbar e v_x v_y B\mathcal{N}+(\Delta+\zeta k_z^2)^2}. \tag{S44}$$

SPECTRAL WEIGHT ANALYSIS

In the main text we determine the spectral weight in the following way:

$$SW = \frac{\omega_p^2}{8} = \int_0^{\omega^*} \sigma_1(\omega) d\omega = \frac{\pi N e^2}{2 m^* V}.$$

This quantity is directly related to the effective band mass m^*. To extract the effective mass, we use $SW \times C \times V_u = N_{eff}$ where N_{eff} is the effective carrier concentration per unit cell, $C = 4.26 \times 10^{14}$ and V_u is the unit cell volume in cm^3. The optically determined N_{eff} is related to the Hall carrier density through $n = N_{eff}/V_u \times m^*$. Here N_{eff} is evaluated for $\omega^* = 5$ meV. $N_{eff} = 0.00455$ for sample A, and 0.044 for sample B.

MAGNETO-OPTICAL TRANSMISSION

In the main text, we determine the band gap using magneto-optical transmission measurements which allow us to follow the energies of Landau level transitions energies in function of magnetic field. Measurements were performed on sample A, at $T = 2$ K, and are shown in Fig. S2.

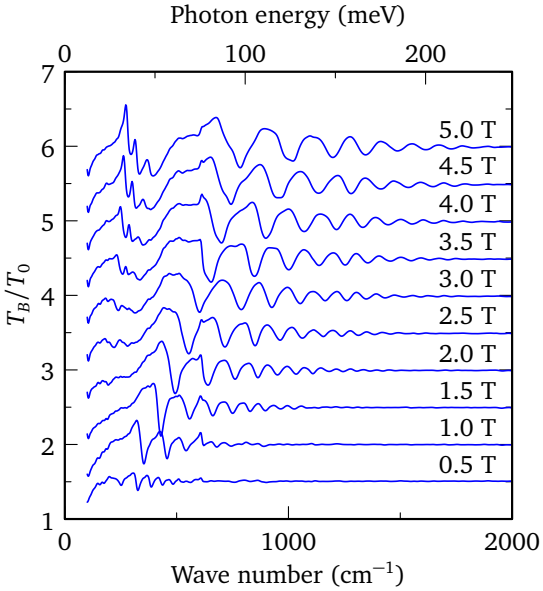

Fig. S2. Magneto-optical transmission for sample A at $T = 2$ K.

OPTICAL CONDUCTIVITY CALCULATED FROM DFT BAND STRUCTURE

The electronic properties of $ZrTe_5$ in the orthorhombic Cmcm (63) phase have been calculated using density functional theory (DFT) with the generalized gradient approximation (GGA) using the full-potential linearized augmented plane-wave (FP-LAPW) method [2] with local-orbital extensions [3] in the WIEN2k implementation [4]. An examination of different Monkhorst-Pack k-point meshes indicated that a $7\times7\times2$ k-point mesh with $R_{mt}k_{max} = 8.25$ was sufficient for good energy convergence. Beginning with the experimental unit cell [5], the total energy was minimized by changing the volume while keeping the c/a ratio constant. The atomic fractional coordinates were then relaxed with respect to the total force, typically resulting in residual forces of less than 0.2 mRy/a.u. per atom. This procedure was repeated until no further improvement was obtained. For both of these procedures spin-orbit coupling is ignored. The final values for the unit cell parameters of $a = 4.06$, $b = 14.76$, and $c = 13.97$ Å are slightly larger than the experimentally-determined values of $a = 3.98$, $b = 14.50$ and $c = 13.72$ Å. The atomic fractional coordinates for Zr, Te1, Te2, and Te3 are determined to be (0.0,0.6847,0.25), (0.0,0.0716,0.1499), (0.0,0.2105,0.5654), and (0.0,0.3352,0.25), respectively,

which are in good agreement with the experimentally-determined values of (0.0,0.6857,0.25), (0.0,0.0701,0.1494), (0.0,0.2099,0.5647), and (0.0,0.3365,0.25).

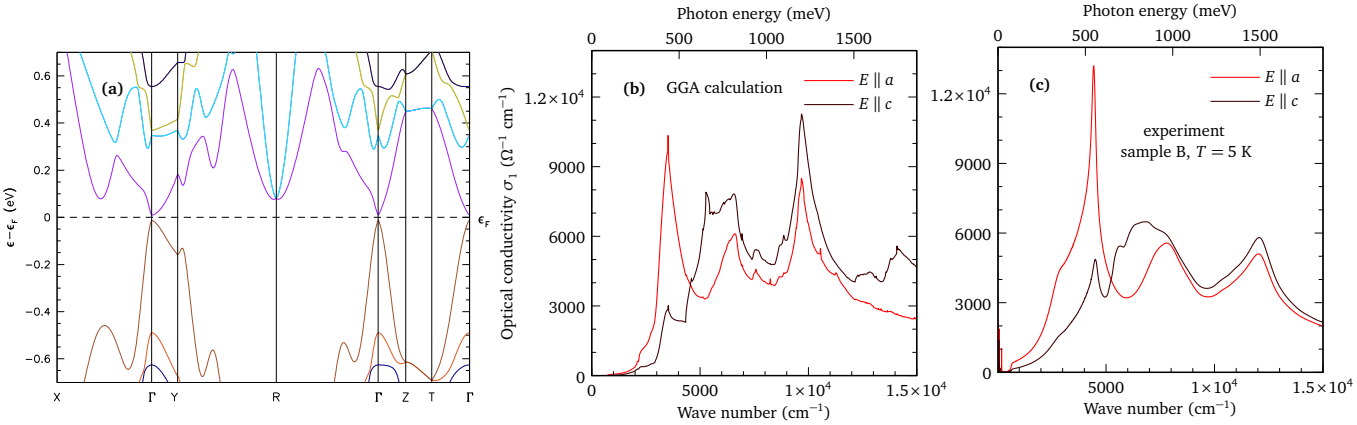

Fig. S3. (a) DFT-calculated band structure in the vicinity of the Fermi level. (b) Optical conductivity determined from the calculated band structure, for the a and c axes. (c) Experimentally determined optical conductivity for light polarized along a and c axes, at $T = 5$K.

The real part of the optical conductivity including the effects of spin orbit coupling has been calculated [6] from the the imaginary part of the dielectric function, $\sigma_{x,x} = 2\pi\omega\,\Im\,\epsilon_{x,x}/Z_0$, using a fine k-point mesh (10 000 k points, yielding a $32 \times 32 \times 9$ mesh); $Z_0 \approx 377\,\Omega$ is the impedance of free space, resulting in units for the conductivity of Ω^{-1}cm^{-1}. In this case, the free-carrier contribution is not calculated, so that the imaginary part of the dielectric function is the sum of the contributions to the dielectric tensor over all the allowed interband transitions. The calculated conductivity is shown along the a and c directions in Fig. S2(a), and is compared to the experimental values at 5 K in Fig. 2(b). The singularities, as well as the general asymmetry in the optical conductivity along the a and c axes are well reproduced, but the peak occurs at a slightly lower energy that is observed experimentally; also, the overall magnitude is lower as well. The conductivity is zero up to about 650 cm^{-1}, above which there is an onset of absorption. This depends on how geometry is optimized. Overall, the calculation agrees very well with the experimental data, both in a and $c-$direction. This means that the singularity at 0.5 eV is indeed van Hove singularity (not excitons for example), and it is two-dimensional.

OPTICAL GAP FROM THE REFLECTANCE DATA

The onset of absorption can be seen directly from the reflectance data, as shown in Fig. S4. The particular measurement shows strong fringes from the Fabry-Perot interference, but only in the transparent regime. The onset of fringes thus corresponds to the onset of absorption at the value of the optical gap or the Pauli blocking. This value also corresponds to half the step in the optical conductivity $\sigma_1(\omega)$. The fringes were observed most likely because that particular sample had split into thin layers during the preparation.

* These authors contributed equally.
† ana.akrap@unifr.ch

[1] G. Eguchi and S. Paschen, Physical Review B **99**, 165128 (2019).
[2] D. J. Singh, *Planewaves, Pseudopotentials and the LAPW method* (Kluwer Adademic, Boston, 1994).
[3] D. Singh, Phys. Rev. B **43**, 6388 (1991).
[4] P. Blaha, K. Schwarz, G. K. H. Madsen, D. Kvasnicka and J. Luitz, WIEN2k, *An augmented plane wave plus local orbitals program for calculating crystal properties* (Techn. Universität Wien, Austria, 2001).
[5] S. Furuseth, L. Brattås, and A. Kjekshus, Acta Chem. Scand. **27**, 2367 (1973).
[6] C. Ambrosch-Draxl and J. O. Sofo, Comp. Phys. Commun. **175**, 1 (2006).

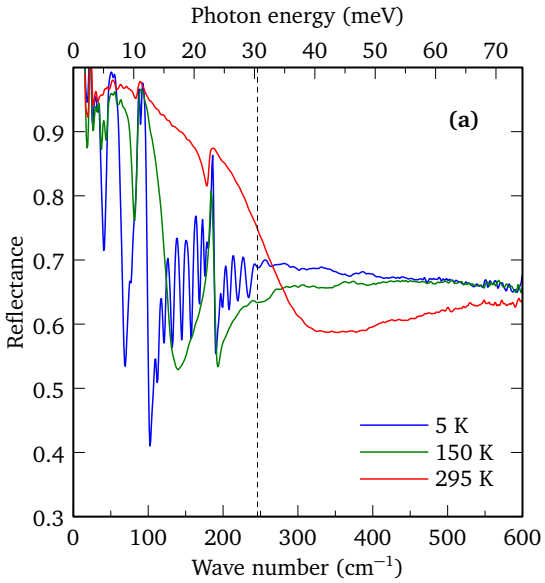

Fig. S4. Optical reflectance showing strong interference fringes, limited to the frequency range below the onset of absorption.